Supplementary Material

Dynamic formation of imidazolidino boronate enables design of cysteine-responsive peptides

Kaicheng Li[1‡], Chelsea Weidman[1‡] and Jianmin Gao[1]*

[1]Department of Chemistry, Merkert Chemistry Center, Boston College,
2609 Beacon Street, Chestnut Hill, MA 02467, United States

[‡]These authors contributed equally to this work

*Correspondence should be addressed to jianmin.gao@bc.edu

Table of Contents **Pages**

1. General methods

L-cysteine, L-serine, L-lysine, glutathione, glucose, 2-formylphenylboronic acid (2-FPBA), and fetal bovine serum were purchased from Fisher Scientific (Pittsburgh, PA). All Fmoc-protected amino acids, HBTU and L-2,3-diaminopropionic acid (L-Dap) were purchased from either Chem-Impex International (Wood Dale, IL) or Advanced Chemtech (Louisville, KY). Fmoc-Rink Amide MBHA resin was purchased from Novabiochem (San Diego, CA). IzB association and dissociation kinetics were studied using a NanoDrop 2000c UV-vis spectrometer. Peptide synthesis was carried out on a Tribute peptide synthesizer (Protein Technologies, Tucson, AZ). Peptide purification was performed on a Waters PrepLC system using a Phenomenex Jupiter C_{18} column (Torrance, CA). ^{1}H NMR spectra were collected using a VNMRS 600 MHz NMR spectrometer with 256 scans at 25 °C. NMR data were processed using MestReNova 11.0 software. Mass spectrometry data were collected using an Agilent 6230 LC TOF mass spectrometer. Phosphate buffer (1 mM) was used for all experiments.

2. NMR studies of 2-FPBA conjugation to L-Dap

To prepare the IzB complex, 315 μL each of 22.2 mM 2-FPBA and L-Dap stock solutions in phosphate buffer were mixed with 70 μL D_2O (10 mM each final concentration, 10% D_2O). The pH was tuned from 1 to 10 incrementally using either 1 N HCl or 1 N NaOH solutions (Figure 2B).

3. IzB complex crystallographic information

300 mM solutions of 2-FPBA (22.5mg in 500 μL) and L-Dap (21.1mg in 500 μL) in water were prepared and combined. 1 mL of MeOH was added to that mixture and the pH was tuned to 7.4 using 1N HCl or 1N NaOH. The solution was filtered through a 0.45 μm PTFE membrane filter (Phenomenex) and allowed to slowly evaporate from a loosely capped 5 mL glass vial at room temperature. After a few days, crystal aggregates were observed and redissolved in pure MeOH. After slow recrystallization at room temperature over a week, single crystals were observed. The structure obtained was a tetramer of IzB complexes around a central NaCl molecule (Table S1, Table S2, Figure S1). The monomer structure can be seen in the main text (Figure 2A).

Table S1. Crystal data and structure refinement for the 2-FPBA-L-Dap IzB complex. Structure seen as a tetramer around a central NaCl molecule.

Identification code	C40H44B4ClN8NaO12	
Empirical formula	C40 H44 B4 Cl N8 Na O12	
Formula weight	930.51	
Temperature	100(2) K	
Wavelength	1.54178 Å	
Crystal system	Tetragonal	
Space group	I4	
Unit cell dimensions	a = 17.4670(5) Å	a= 90°.
	b = 17.4670(5) Å	b= 90°.
	c = 6.7244(2) Å	g = 90°.
Volume	2051.59(13) $Å^3$	
Z	2	
Density (calculated)	1.506 Mg/m^3	
Absorption coefficient	1.580 mm^{-1}	
F(000)	968	
Crystal size	0.250 x 0.220 x 0.140 mm^3	
Theta range for data collection	5.064 to 66.529°.	
Index ranges	-20<=h<=11, -20<=k<=19, -7<=l<=7	
Reflections collected	5002	
Independent reflections	1718 [R(int) = 0.0245]	
Completeness to theta = 66.529°	99.3 %	
Absorption correction	Semi-empirical from equivalents	
Max. and min. transmission	0.7528 and 0.6716	
Refinement method	Full-matrix least-squares on F^2	
Data / restraints / parameters	1718 / 1 / 163	
Goodness-of-fit on F^2	1.039	
Final R indices [I>2sigma(I)]	R1 = 0.0227, wR2 = 0.0577	
R indices (all data)	R1 = 0.0232, wR2 = 0.0580	
Absolute structure parameter	0.032(8)	
Extinction coefficient	n/a	
Largest diff. peak and hole	0.305 and -0.156 $e.Å^{-3}$	

Table S2. Atomic coordinates (x 10^4) and equivalent isotropic displacement parameters ($Å^2$x 10^3) for the 2-FPBA-L-Dap IzB complex. U(eq) is defined as one third of the trace of the orthogonalized U^{ij} tensor.

	x	y	z	U(eq)
Na(1)	5000	5000	2511(3)	15(1)
Cl(1)	5000	5000	6570(1)	14(1)
O(1)	6341(1)	5315(1)	2576(2)	13(1)
O(2)	7024(1)	5597(1)	5578(2)	13(1)
O(3)	6905(1)	5644(1)	8865(2)	16(1)
N(1)	6699(1)	4269(1)	5014(3)	12(1)
N(2)	7501(1)	3290(1)	6337(3)	17(1)
B(1)	6941(1)	5046(1)	3834(4)	12(1)
C(1)	6914(1)	5280(1)	7325(3)	12(1)
C(2)	6810(1)	4422(1)	7171(3)	14(1)
C(3)	7529(1)	3942(1)	7708(4)	17(1)
C(4)	7248(1)	3617(1)	4474(4)	15(1)
C(5)	7877(1)	4011(1)	3306(3)	13(1)
C(6)	8536(1)	3643(1)	2655(3)	16(1)
C(7)	9065(1)	4057(1)	1550(4)	20(1)
C(8)	8937(1)	4828(1)	1137(3)	18(1)
C(9)	8280(1)	5192(1)	1808(3)	14(1)
C(10)	7735(1)	4783(1)	2899(3)	12(1)

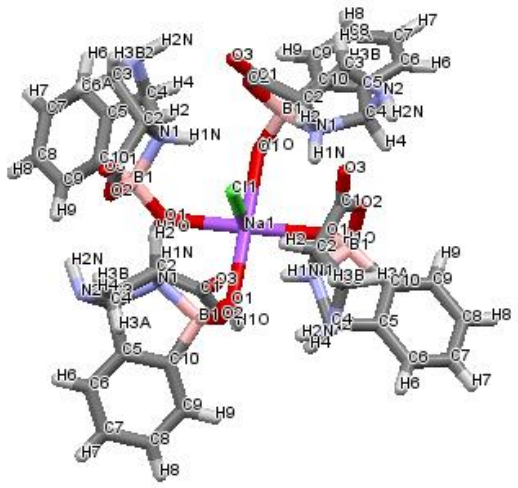

Figure S1. Crystal structure of the tetrameric NaCl salt IzB complex between 2-FPBA and L-Dap.

4. Association of 2-FPBA and 1,2-ethylenediamine

IzB complex formation was studied using 1,2-ethylenediamine, a readily available simple diamine, to examine the broad applicability to 1,2-diamines. An equimolar solution of 2-FPBA and 1,2-ethylenediamine in phosphate buffer was prepared (9 mM each final concentration, 10% D_2O). The pH was tuned to 8 using either 1 N HCl or 1 N NaOH solutions. The reaction proceeded rapidly to afford an IzB complex, similar to 2-FPBA and L-Dap, giving a benzylic H peak at 5.6 ppm (Figure S2). The reaction proceeds instantaneously, reacting too quickly to measure the kinetics via UV-vis.

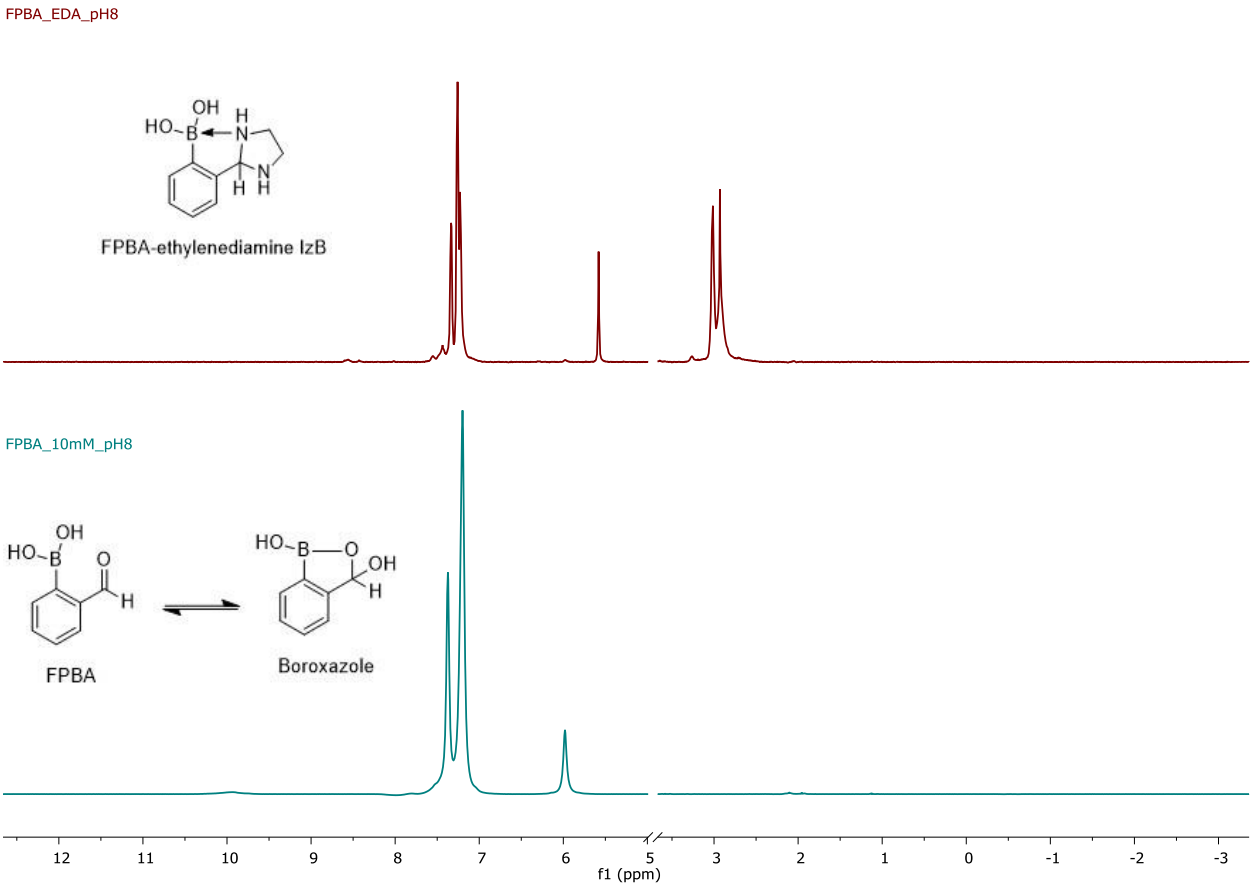

Figure S2. ^{1}H NMR of IzB conjugation with 2-FPBA and ethylenediamine at pH 8 (top) compared to 2-FPBA alone (bottom). The FPBA peak around 6.0 ppm indicates boroxazole formation (see Cal et al., *J. Am. Chem. Soc.* **2012**, *134* (24), 10299).

5. Kinetic and thermodynamic studies of the IzB complex formation

Both the association and dissociation kinetics were examined via UV-vis absorption. The disappearance or appearance of the characteristic 2-FPBA absorbance at 254 nm was used to measure the formation or breakdown of the IzB complex, respectively. Data were collected after blank subtraction using phosphate buffer (1 mM, pH 7.4). The reactions were performed in a quartz cuvette (10 mm path length, total volume

~1 mL) using phosphate buffer at room temperature. All stock solutions were prepared in phosphate buffer (pH 7.4).

For the association reaction, 6 µL of 2-FPBA stock (10 mM) was added to 994 µL phosphate buffer in the cuvette and mixed to make a 60 µM 2-FPBA solution. The absorbance spectrum was recorded as the initial time point. 1.2 µL of L-Dap stock (50 mM) was added to the cuvette and quickly mixed via pipetting. The absorbance profile was recorded approximately every 3 seconds. A rapid decrease in absorbance at 254 nm was seen as the FPBA was converted to the IzB complex, which does not have an absorbance maximum at 254 nm. Plotting the time versus absorbance at 254 nm followed by curve fitting gave the forward reaction time constant (Figure S3).

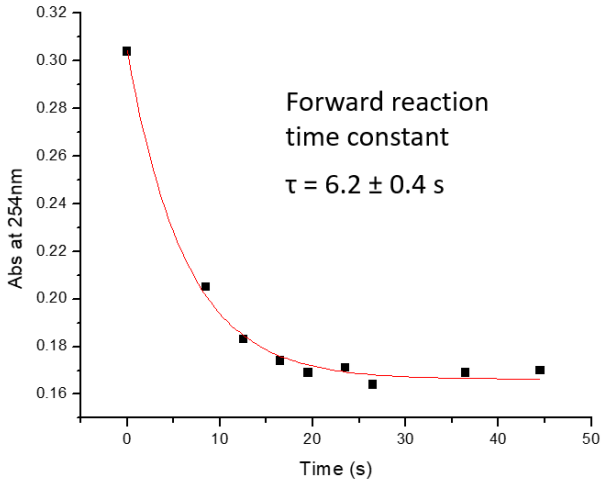

Figure S3. Association kinetics of 2-FPBA and L-Dap to form the IzB complex.

As the reactants were used at equal concentrations, the forward reaction kinetics data were fitted according to the equations of second order relaxation kinetics (details can be found on Page 369 of *Physical Chemistry: Principles and Applications in Biological Sciences*, Fourth Edition, by Tinoco et al., Prentice Hall PTR, 2001). The following equations were used to calculate the relaxation constant (τ): equation 1 describes the reaction mechanism, equation 2 describes the second order relaxation kinetics, equation 3 defines τ, equations 4-7 relate the concentration of reactants at equilibrium ([$\bar{A}$] and [$\bar{B}$]), K_d, and reaction rates (k_1 and k_{-1}).

[1] $A + B \underset{k_{-1}}{\overset{k_1}{\rightleftharpoons}} P$

[2] $y = y_0 + Ae^{(-t/\tau)}$

[3] $\tau = \dfrac{1}{k_{-1} + k_1([\bar{A}] + [\bar{B}])}$

[4] $[\bar{A}] = [\bar{B}]$

[5] $[\bar{A}] + [\overline{AB}] = 6 \times 10^{-5}$ M (total reactant concentration)

[6] $K_d = \dfrac{[\bar{A}][\bar{B}]}{[\overline{AB}]} = 10^{-4}$ M (Figure 2D)

[7] $K_d = \dfrac{k_{-1}}{k_1} = 10^{-4}$ M

For the dissociation reaction, an equimolar mixture of 2-FPBA and L-Dap (1 mM) was created by mixing 90 μL of 2-FPBA stock (10 mM) and 18 μL of L-Dap stock (50 mM) with 792 μL phosphate buffer. The mixture was incubated at room temperature for 15 minutes to allow the IzB complex to form completely. The mixture was diluted 16.7x to a final concentration of 60 μM and quickly mixed via pipetting. The absorbance profile was recorded approximately every 3 seconds. The initial absorbance value of the IzB complex was obtained from a separate equimolar mixture of 2-FPBA and L-Dap (600 μM) pre-incubated for 15 minutes. The absorbance at 254 nm was obtained via NanoDrop reading. A 600 μM solution measured using a 1 mm pat/h length would be equivalent to a 60 μM solution measured using a 10 mm path length. A rapid increase in absorbance at 254 nm was seen as 2-FPBA was generated upon dissociation of the IzB complex. Plotting the absorbance at 254 nm against time followed by curve fitting gave the relaxation time constant of the backward reaction (Figure 2C).

For the equilibrium binding study, increasing amounts of a L-Dap stock (100 mM) was added to an FPBA solution (50 μM) to give final L-Dap concentrations of 100 μM to 900 μM. The decrease in absorbance at 254 nm was measured as the 2-FPBA was converted to the IzB complex. Plotting the absorbance at 254 nm against the concentration of L-Dap gave the binding curve shown in Figure 2D. Fitting the data to a hyperbola equation ($y = A + Bx/(C + x)$) yielded the apparent K_d value ($K_d = C$) shown in Figure 2D.

6. Probing small molecule interference of IzB formation via NMR

100 μL of 2-FPBA-L-Dap IzB complex (10 mM) was diluted in 400 μL phosphate buffer (pH 7.4, 20% D_2O). The solution was mixed with 500 μL stock solutions of lysine (20 mM), serine (20 mM), glutathione (20 mM), glucose (20 mM), and cysteine (2 mM) in phosphate buffer (Figure 3). The pH of the mixtures was tuned to 7.4 using 0.5N HCl or 0.5N NaOH. All samples were incubated for 30 minutes before the ^{1}H-NMR spectra were taken.

7. pH-dependent cyclization of KL21

A solution of KL21 peptide (500 μM) in phosphate buffer (20% D_2O) was prepared. The pH was tuned from 2.5 to 7.4 incrementally using either 0.5N HCl or 0.5N NaOH solutions. Cyclization was monitored by the disappearance of the 2-FPBA aldehyde peak at 9.8 ppm and the appearance of the IzB benzylic hydrogen peak around 5.8 ppm (Figure S4).

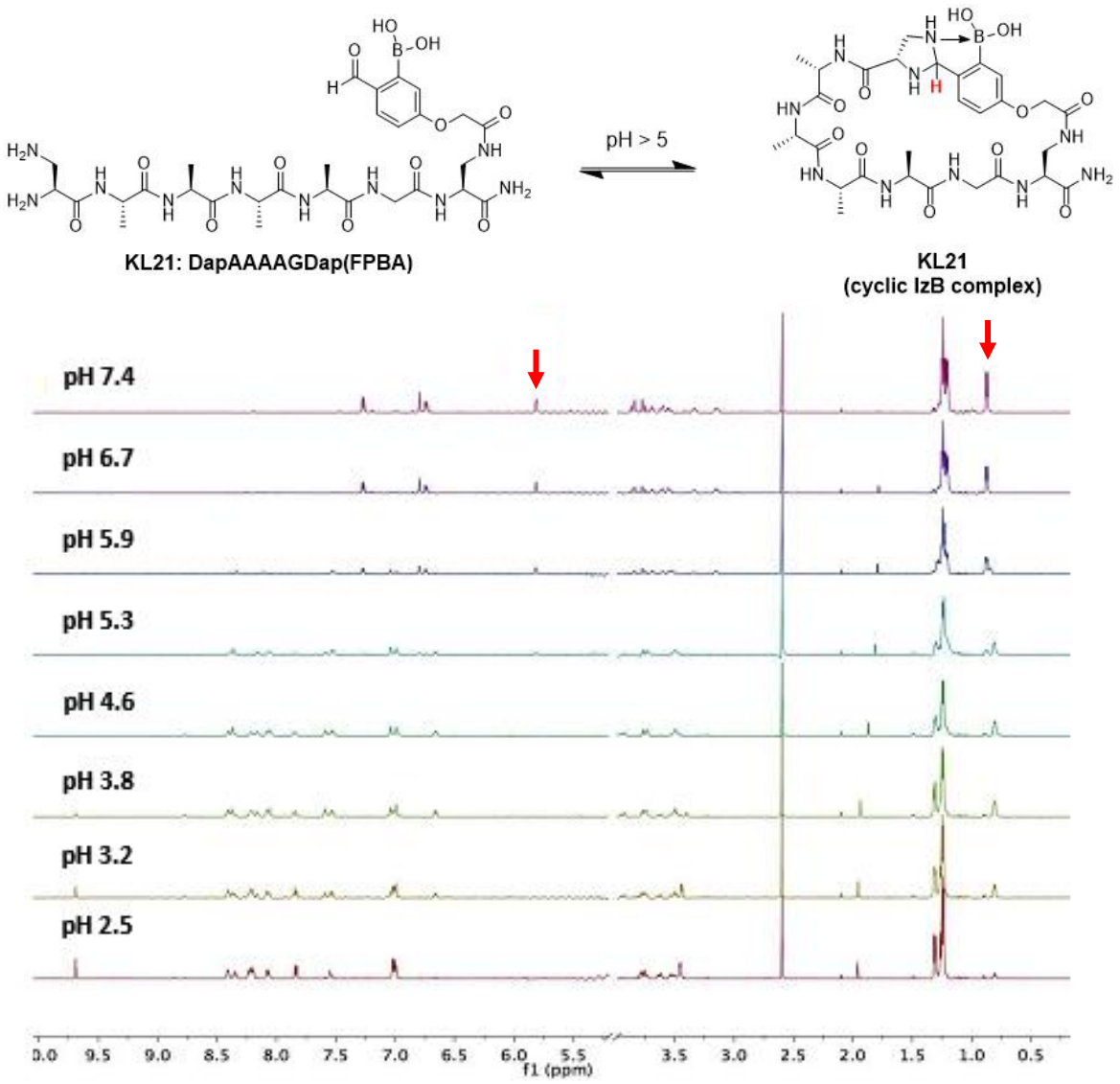

Figure S4. ^{1}H-NMR characterization of KL21 cyclization at varied pH. The IzB signature peak around 5.8 ppm, as well as an up-field shifted methyl peak (one of the Ala side chains) are highlighted with red arrows.

8. Probing small molecule interference of KL21 cyclization via NMR

0.15 mg KL21 peptide was dissolved in 900 µL phosphate buffer (pH 7.4, 20% D_2O, final KL21 concentration: 200 µM). The solution was mixed with 100 µL stock solutions of lysine (20 mM), serine (20 mM), glutathione (20 mM) and glucose (20 mM) in phosphate buffer (Figure S5). The pH of the mixtures was tuned to 7.4 using 0.5 N HCl or 0.5 N NaOH. The samples were incubated for 30 minutes before the NMR spectra were taken.

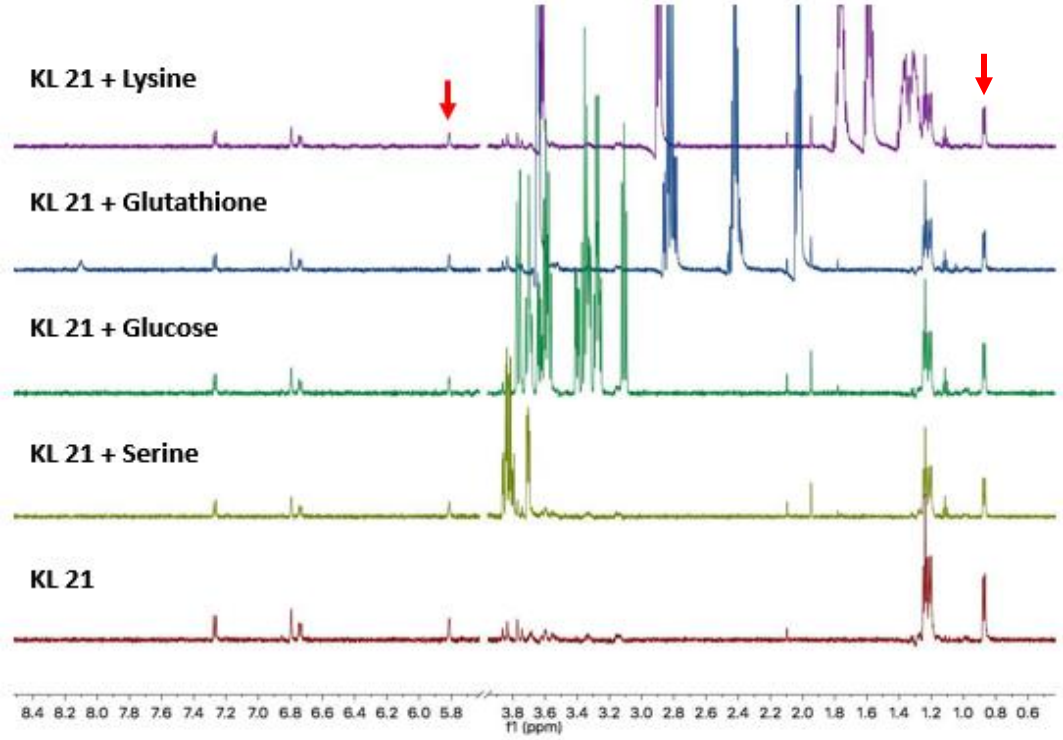

Figure S5. ^{1}H-NMR data showing the lack of small molecule interference of KL21 cyclization. The IzB signature peak around 5.8 ppm, as well as an up-field shifted methyl peak (one of the Ala side chains) are highlighted with red arrows.

9. Cysteine-induced KL21 linearization

0.15 mg KL21 peptide was dissolved in 800 µL phosphate buffer (pH 7.4, 20% D_2O, final KL21 concentration: 200 µM). Increasing amounts of a cysteine stock (100 mM) in phosphate buffer was added to give final cysteine concentrations of 100 µM to 4 mM (Figure 4C). To ensure the cysteine remained reduced, iTCEP (25 µL) was added to the NMR tube. The pH of the mixture was tuned to 7.4 using 0.5 N HCl or 0.5 N NaOH. A titration curve was generated by plotting the peak area of the two TzB benzylic proton peaks against cysteine concentration. Fitting this titration curve using a hyperbola equation gave the EC_{50} value for cysteine-induced KL21 linearization (Figure S6).

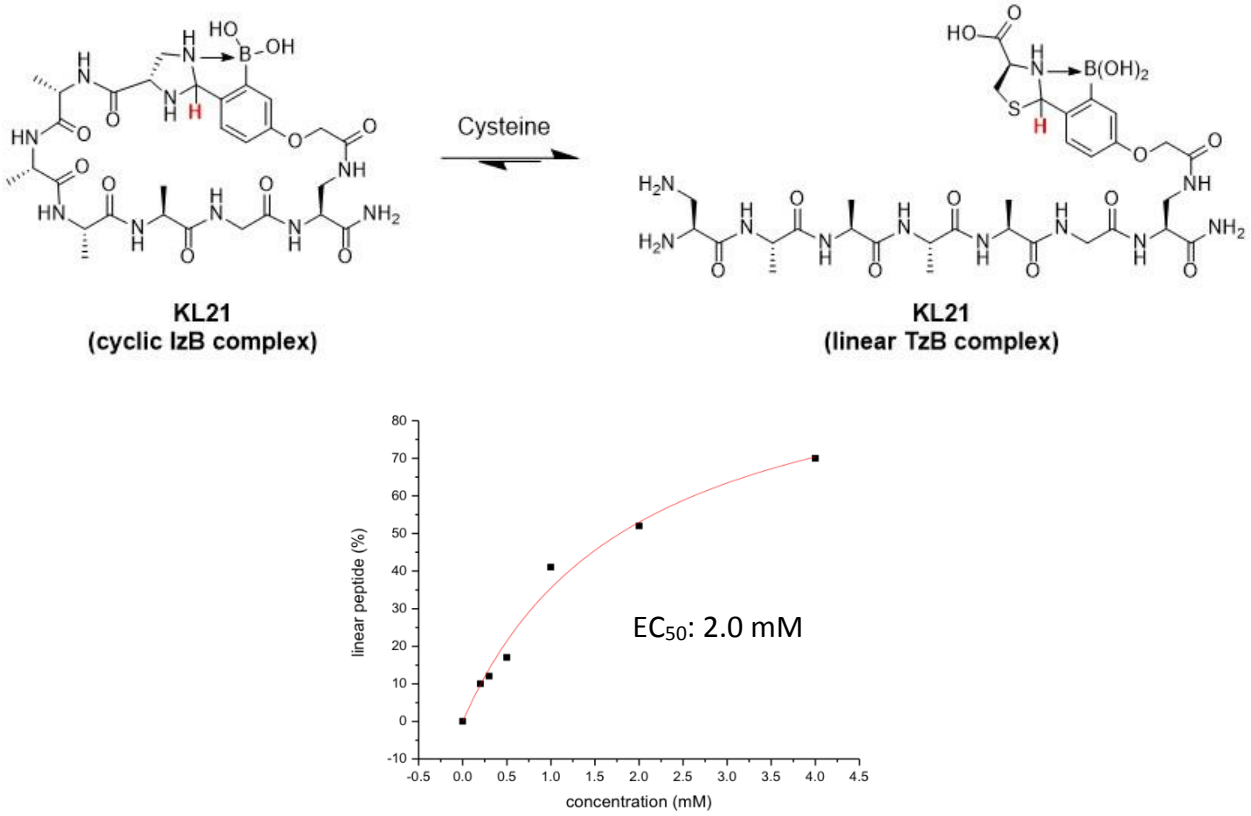

Figure S6. Scheme and titration curve of cysteine-induced linearization of KL21 in PBS buffer.

10. Cysteine-induced KL21 linearization in fetal bovine serum (FBS)

To a solution of KL21 peptide (200 μM) in 900 μL phosphate buffer (pH 7.4, 20% D_2O) and 100 μL FBS, increasing amounts of a cysteine stock (100 mM) in phosphate buffer was added to give final cysteine concentrations of 100 μM to 4 mM (Figure S7). To ensure the cysteine remains reduced, iTCEP (25 μL) was added to the NMR tube. The pH of the mixtures was tuned to 7.4 using 0.5 N HCl or 0.5 N NaOH. All samples were incubated for 30 minutes before the ^{1}H-NMR spectra were taken.

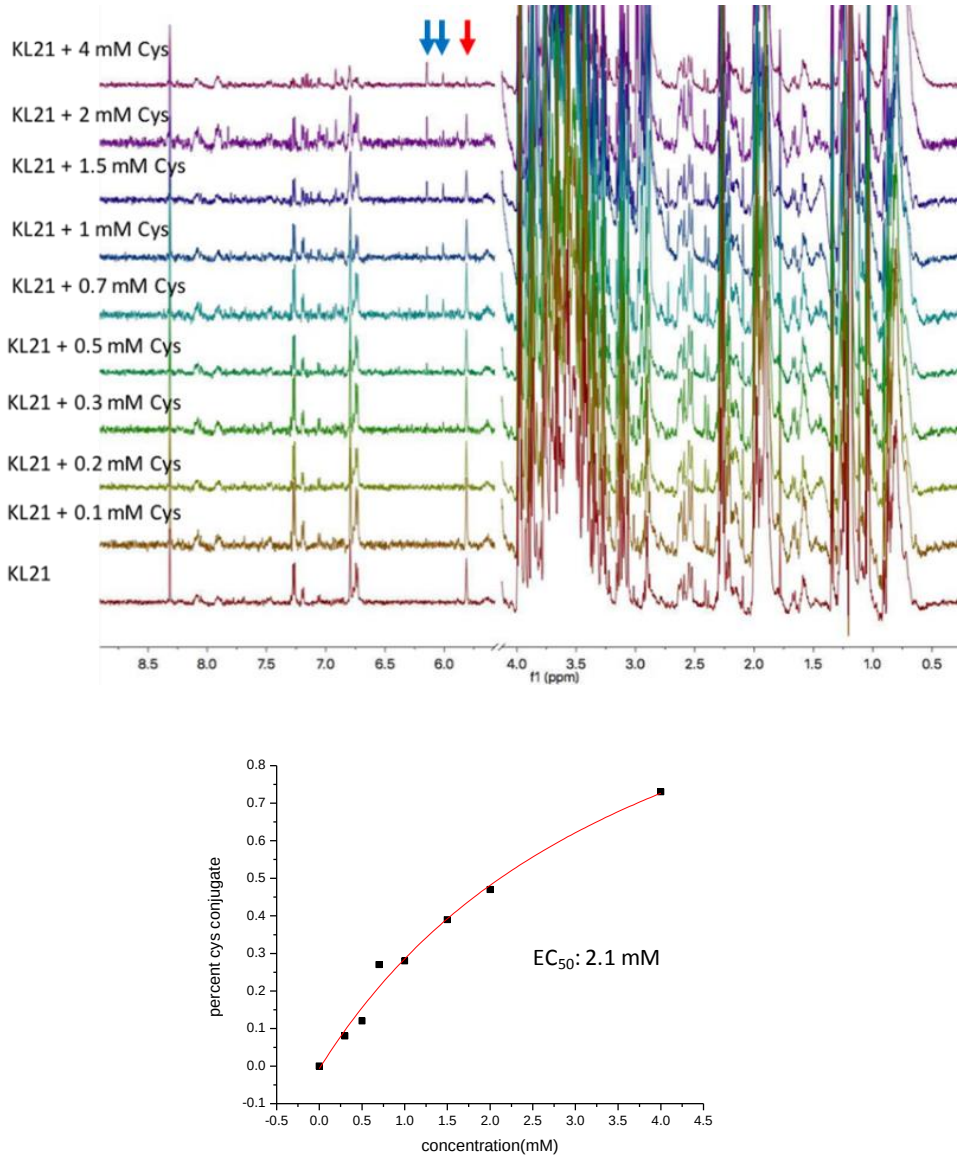

Figure S7. KL21 reports the gradual titration of cysteine in the presence of 10% FBS. The red and blue arrows denote the IzB and TzB benzylic hydrogen(s) respectively. These peaks saw minimal interference by NMR resonances of FBS.

11. KL21 reports on cysteine oxidation in FBS

A solution of KL21 peptide (200 μM) and cysteine (4 mM) in 1.8 mL phosphate buffer (pH 7.4, 20% D_2O) with 200 μL fetal bovine serum was made and a ^{1}H-NMR spectrum was recorded as soon as possible (~30 minutes). The solution (~2 mL) was incubated at 25°C in a scintillation vial open to air to allow gradual cysteine oxidation over time. The ^{1}H-NMR spectrum was recorded occasionally over the course of a few days (Figure S8).

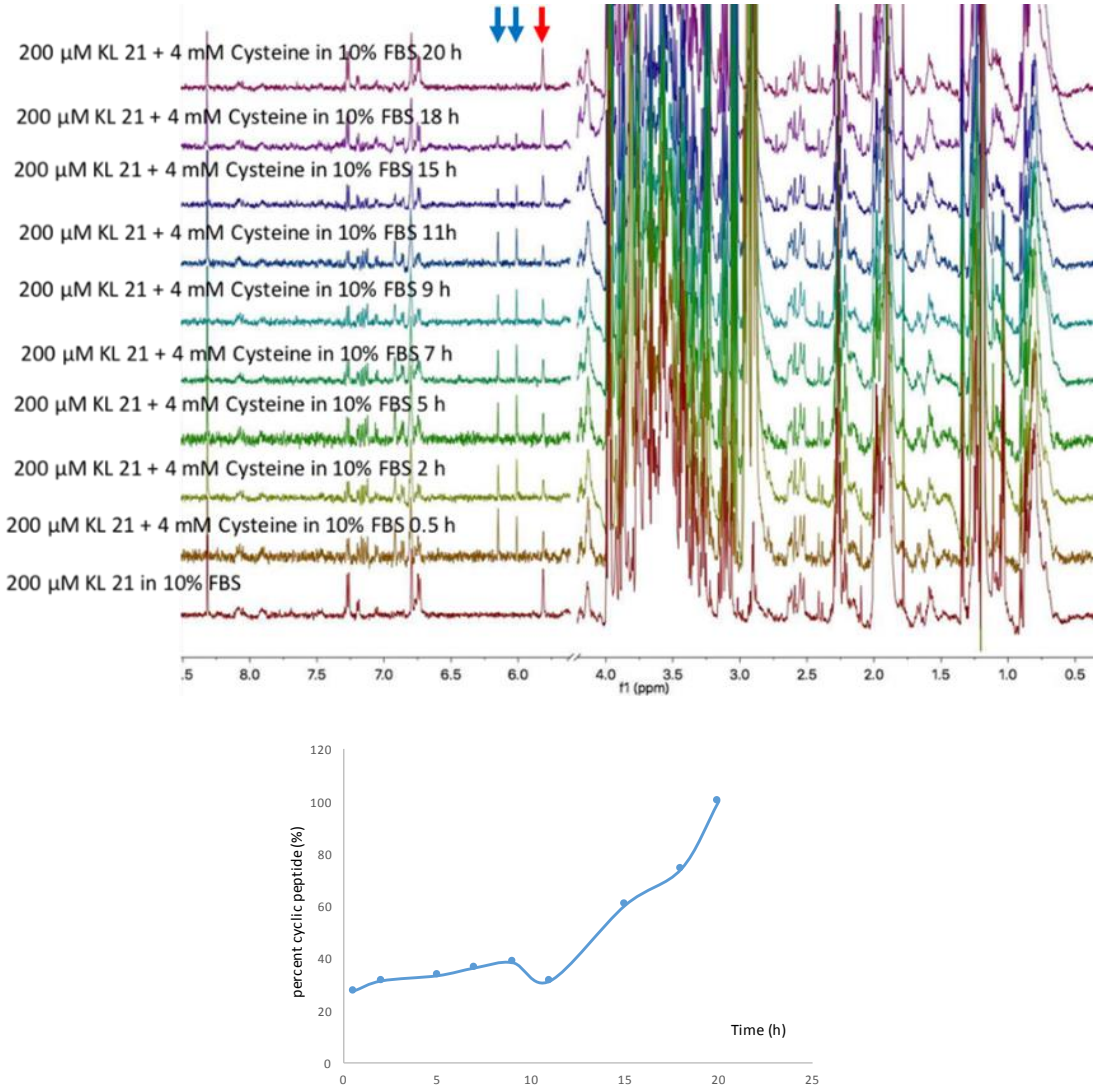

Figure S8. ^{1}H-NMR spectra of KL21 reveals cysteine oxidation over time in FBS. The red and blue arrows denote the IzB and TzB benzylic hydrogen(s) respectively. Integration of these peaks allows estimation of the cyclic peptide percentage over time, the plot of which is shown underneath the NMR spectra.

12. Attempts at incorporating fluorophore-quencher pairs into a peptide

Inspired by the IzB conjugation of KL21, development of a single-peptide based fluorogenic assay was attempted by incorporation of dabcyl and fluorescein near the N- and C-termini, respectively. Peptides of various lengths were synthesized to include 5, 8, or 10 residues between fluorescein and dabcyl (Figure S9). Addition of cysteine to the cyclized peptides did not show significant increase in fluorescence, indicating no significant change in distance between fluorescein and dabcyl.

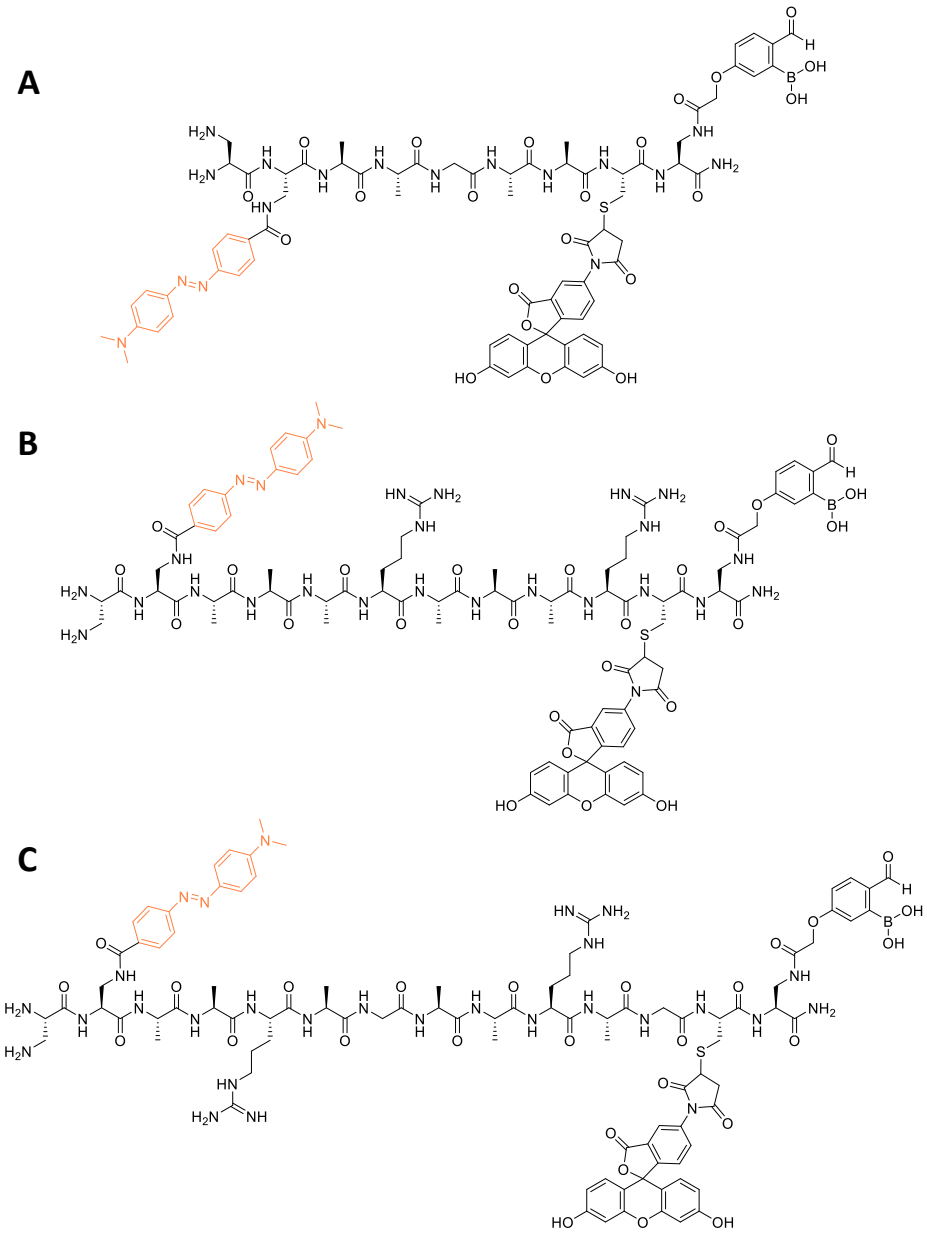

Figure S9. Previous attempts of developing a fluorophore-quencher pair incorporated into a peptide. Peptides of various lengths incorporating 5 (A), 8 (B), or 10 (C) residues between the fluorophore-quencher pair were explored. No fluorescence increase was observed upon cysteine titration.

13. KL22 and KL23: fluorogenic cysteine sensors

To increase the distance between the fluorophore and quencher, two separate peptides were made to either incorporate the fluorophore or quencher. The concentration of KL22 (2 L-Dap residues and fluorescein), KL23 (2-FPBA moieties and dabcyl), and free dabcyl acid were measured by absorbance at 495 nm, 453 nm, and 453 nm in PBS buffer (pH 7.4), respectively. The stock concentrations were determined to be 15 μM, 6 μM, and 30 μM accordingly.

Determination of the dissociation constant between KL22 and KL23

Samples were prepared in 96-well plate, each sample being 150 μL and pre-mixed. The final concentration of KL22 is 0.1 μM. The fluorescence was excited at 495 nm and measured at 517 nm. Fitting this data using a hyperbola equation gave the K_d of KL22 and KL23 dissociation (Figure S10).

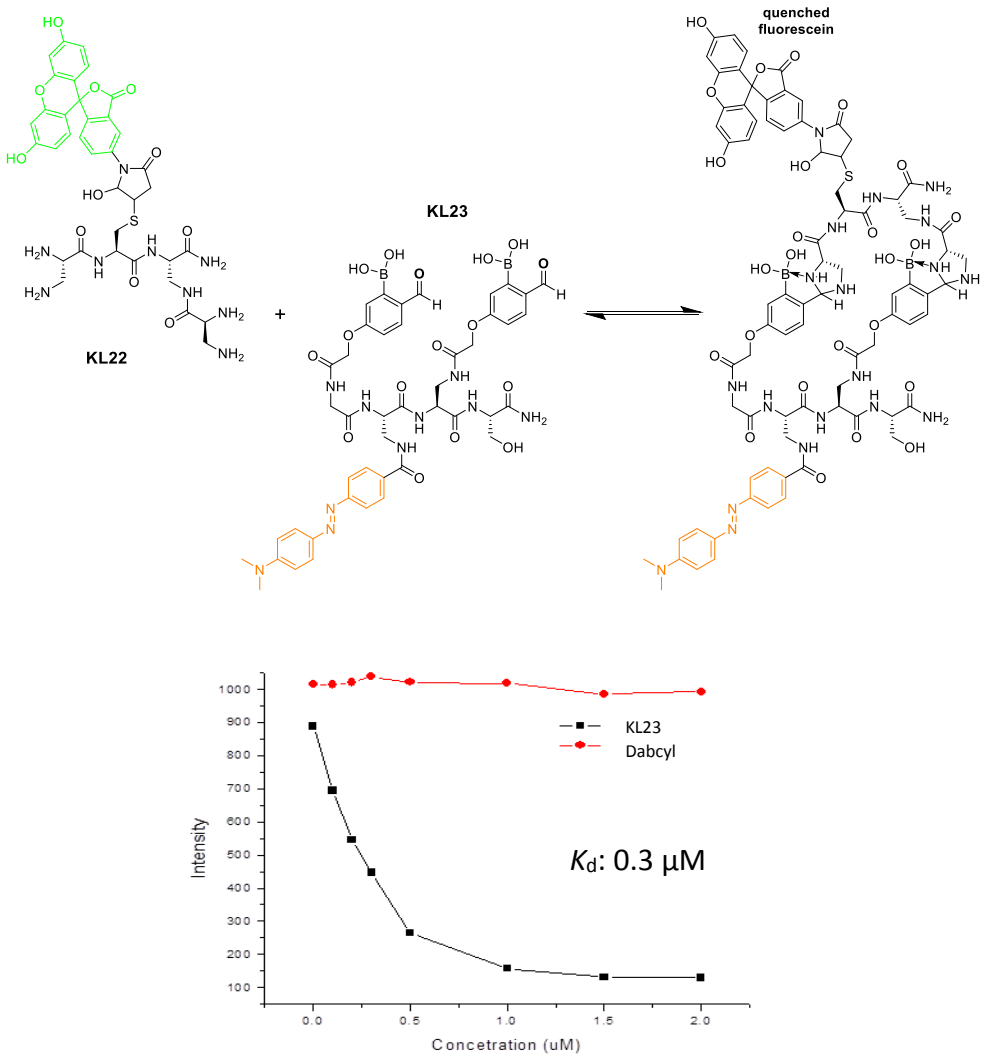

Figure S10. Fluorescence quenching of KL22 with KL23 and free dabcyl.

Determination of the cysteine EC_{50} value with KL22 and KL23 IzB conjugate

Samples were prepared in 96-well plate, each sample being 150 μL and pre-mixed. The final concentration is 0.1 μM KL22 with 1 μM KL23. The small molecule stock solutions were 10 mM each. Fluorescence excitation was set at 495 nm and measured at 517 nm. Fitting this data using a hyperbola equation gave the EC_{50} of cysteine-induced quenched KL22-23 IzB conjugate dissociation (Figure 4D).

14. KL22-23 cysteine sensing in FBS

Samples were prepared in 96-well plate, each sample being 150 μL and pre-mixed. The final concentration is 0.1 μM KL22 with 1 μM KL23. The cysteine stock solution was 10 mM. Fluorescence excitation was set at 495 nm and measured at 517 nm. The data were normalized and fitted using a hyperbola equation to give the EC_{50} of cysteine-induced quenched KL22-23 IzB conjugate dissociation (Figure S11).

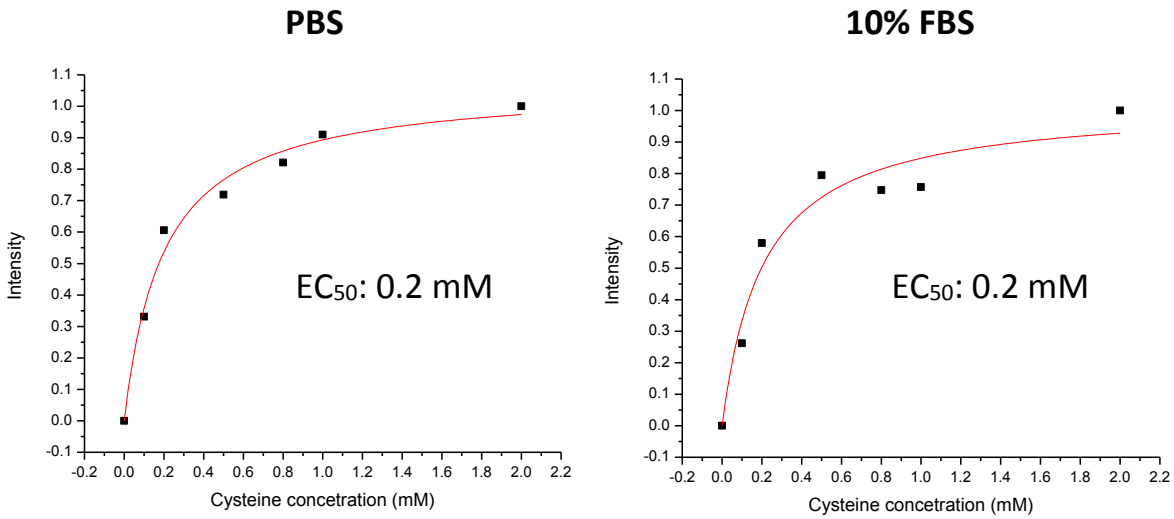

Figure S11. Normalized cysteine titration with KL22-23 IzB complex in PBS or 10% FBS.

15. Synthesis and characterization of the carboxylic acid derivative of 2-FPBA

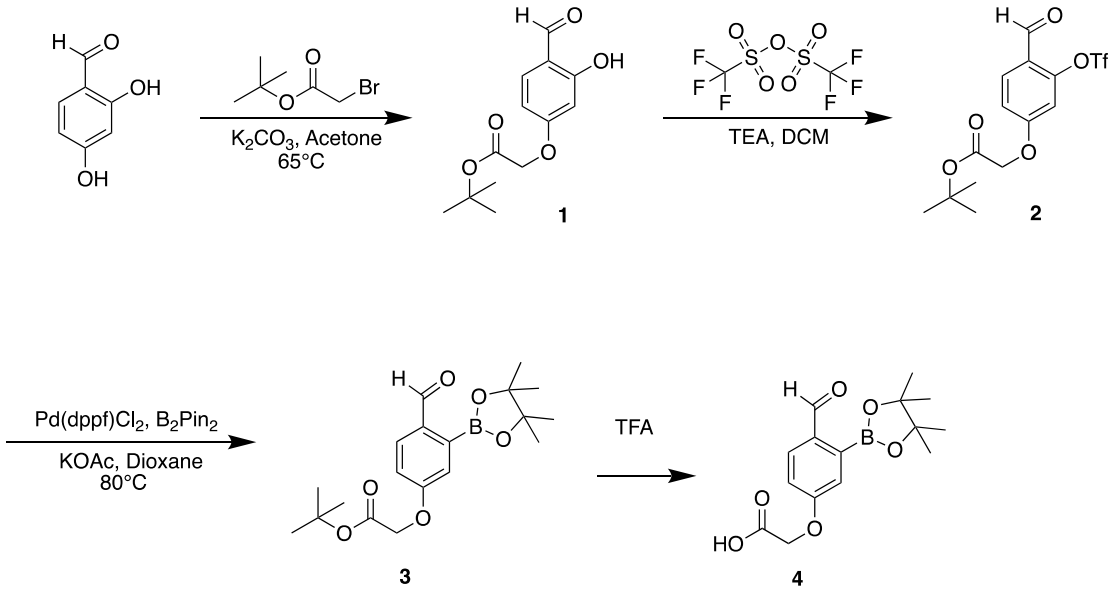

Scheme S1. Synthetic route for the carboxylic acid derivative of 2-FPBA.

Synthesis of **1**

2,5-dihydroxylbenzaldehyde (3.00 g, 21.74 mmol) was dissolved in 10 mL acetone, to which tert-butyl 2-bromoacetate (4.24 g, 21.43 mmol) and potassium carbonate (5 g, 36.23 mmol) was added. The reaction was stirred at 65 ℃ for 16 h then cooled down to room temperature. 150 mL of water was added to the reaction mixture and extracted with ethyl acetate (3×150 mL). The organic layers were combined, washed with brine (150 mL) and dried over sodium sulfate. Ethyl acetate was evaporated and the crude product was purified by silica column using ethyl acetate: hexane (1:10) to yield a white solid (2.90 g, 53%).

^{1}H-NMR (500 MHz, Chloroform-*d*) δ 11.42 (s, 1H), 9.72 (s, 1H), 7.44 (d, *J* = 8.7 Hz, 1H), 6.56 (d, *J* = 11.1 Hz, 1H), 6.36 (d, *J* = 2.4 Hz, 1H), 4.55 (s, 2H), 1.48 (s, 9H).
^{13}C-NMR (126 MHz, Chloroform-*d*) δ 194.47, 166.81, 164.88, 164.25, 135.37, 115.70, 108.45, 101.45, 82.97, 65.48, 28.00.
MS-ESI^{+}: *m/z* calculated for $C_{13}H_{17}O_5$ $[M+H]^+$ 253.1076, observed 253.1055.

Synthesis of **2**

1 (1.51 g, 6.00 mmol) and triethylamine (3.03 g, 30.00 mmol) were dissolved in 15 mL of dichloromethane and stirred at -78 ℃ for 5 min. Trifluoromethanesulfonic anhydride (3.39 g, 12.00 mmol) was added slowly into the mixture over 1 min. The reaction was then allowed to stir at room temperature for 1 h under argon and quenched with 50 mL of saturated sodium bicarbonate. The mixture was stirred for 5 min and then extracted with dichloromethane (3×100 mL). The combined organic layer was washed with brine (100 mL) and dried over sodium sulfate. After solvent removal, the crude product was purified by silica column using ethyl acetate: hexane (1:9) to yield a light yellow solid (1.90 g, 83%).

^{1}H-NMR (600 MHz, Chloroform-*d*) δ 10.13 (s, 1H), 7.94 (d, *J* = 8.7 Hz, 1H), 7.00 (dd, *J* = 8.7, 2.3 Hz, 1H), 6.88 (d, *J* = 2.3 Hz, 1H), 4.61 (s, 2H), 1.49 (s, 9H).
^{13}C-NMR (151 MHz, Chloroform-*d*) δ 187.90, 168.90, 166.14, 153.79, 134.82, 125.08, 121.24, 117.31, 111.52, 86.14, 68.56, 30.66.
MS-ESI^{+}: *m/z* calculated for $C_{14}H_{16}F_3O_7S$ $[M+H]^+$ 385.0569, observed 385.0515.

Synthesis of **3**

2 (1.50g, 3.90 mmol), B_2Pin_2 (2.57g, 10.12 mmol), $Pd(dppf)Cl_2$ (300 mg, 0.41 mmol) and potassium acetate (2.00 g, 21.01 mmol) were dissolved in 10 mL of anhydrous dioxane, to which ~100 mg of 3 Å molecular sieves were added. The reaction was flushed with argon for 15 min and allowed to stir for 1 h at 80 °C. The reaction was cooled down to room temperature and water (50 mL) was added to the reaction. The product was extracted with ethyl acetate (3×100 mL). The combined organic layer was washed with brine (100 mL) and dried over sodium sulfate. Ethyl acetate was removed and the product was purified on silica gel column using ethyl acetate: hexane (3:17) to give the desired product a white solid (0.54 g, 38% yield).

^{1}H-NMR (600 MHz, Chloroform-*d*) δ 10.40 (s, 1H), 7.93 (d, *J* = 8.6 Hz, 1H), 7.28 (d, *J* = 2.6 Hz, 1H), 7.03 (dd, *J* = 8.6, 2.7 Hz, 1H), 4.59 (s, 2H), 1.48 (s, 9H), 1.37 (s, 12H).
^{13}C-NMR (151 MHz, Chloroform-*d*) δ 195.67, 169.89, 164.09, 138.03, 132.95, 123.06, 119.73, 87.11, 85.40, 68.22, 30.65, 27.50.
MS-ESI^{+}: *m/z* calculated for $C_{13}H_{16}BO_5$ $[M\text{-}Pin\text{-}H_2O+H]^+$ 263.1091, observed 263.1221.

Synthesis of **4**

3 (200 mg, 0.55 mmol) was dissolved in 2 mL of dichloromethane and stirred at 0 °C, to which 3 mL of trifluoroacetic acid (TFA) was added. The mixture was stirred at room temperature for 1 h before the dichloromethane and TFA were evaporated. The residue was treated with 5 mL of TFA for another hour at room temperature. Removing TFA completely via evaporation and washing with toluene and dichloromethane yielded an off-white powder as the desired product (150 mg, 89%).

^{1}H NMR (600 MHz, DMSO-d_6) δ 13.12 (s, 1H), 10.13 (s, 1H), 7.87 (d, *J* = 8.5 Hz, 1H), 7.16 – 7.10 (m, 2H), 4.82 (s, 2H), 1.32 (s, 12H).
^{13}C NMR (151 MHz, DMSO-d_6) δ 195.33, 172.74, 164.62, 137.18, 134.51, 123.14, 119.16, 87.21, 67.67, 27.77.
MS-ESI^{+}: *m/z* calculated for $C_{13}H_{16}BO_5$ $[M\text{-}Pin\text{-}H_2O+H]^+$ 207.0465, observed 207.0422.

16. Peptide synthesis and characterization

KL21

KL21 (DapAAAAGDap(FPBA)) was synthesized using standard Fmoc-based SPPS on Rink Amide MBHA resin. It was carried out on a 0.05 mmol synthesis using 5 equivalents of each amino acid and 4.75 equivalents of HBTU for each coupling reaction. $Pd(PPh_3)_4$ (100 mg) and phenylsilane (600μL) in dichloromethane (2 mL) was added to the resin to selectively deprotect the Alloc group. The 2-FPBA functionality was installed by activating **4** (4 eq) with HBTU (3.8 eq) in 0.4M *N*-methylmorpholine in dimethylformamide for about 5 minutes, then adding the solution to the peptide on-resin and mixing for 1h.

After N-terminal Fmoc deprotection with 20% piperidine in dimethylformamide, KL21 was cleaved off resin and globally deprotected with 85% trifluoroacetic acid : 5% H_2O : 5% phenol : 5% thioanisole treatment for 2 hours. Cold ether precipitation yielded crude peptide, which was purified using RP-HPLC (Scheme S2). Peptide purity was assessed by ^{1}H NMR and LCMS. The calculated m/z $[M+H]^+$ is 737.3384 and the observed m/z $[M+H]^+$ is 737.3388 (Figure S12).

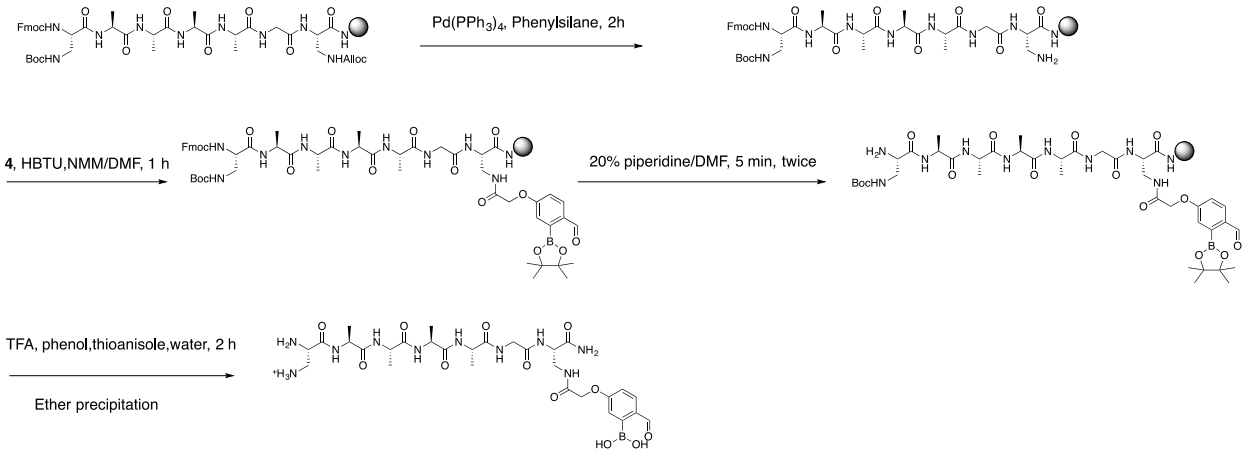

Scheme S2. Synthetic route for KL21.

For LCMS analysis, an Agilent Extend C18 (1.8 µm, 2.1 x 50 mm) analytical column was used with a water-acetonitrile mobile phase at a flow rate of 0.2 mL/min. The gradient used was as follows: isocratic 5% CH_3CN for 5 min, gradient from 5% to 95% CH_3CN in 10 min, isocratic 95% CH_3CN for 5 min, gradient from 95% to 5% CH_3CN in 1 min, then isocratic 5% CH_3CN for 5 min.

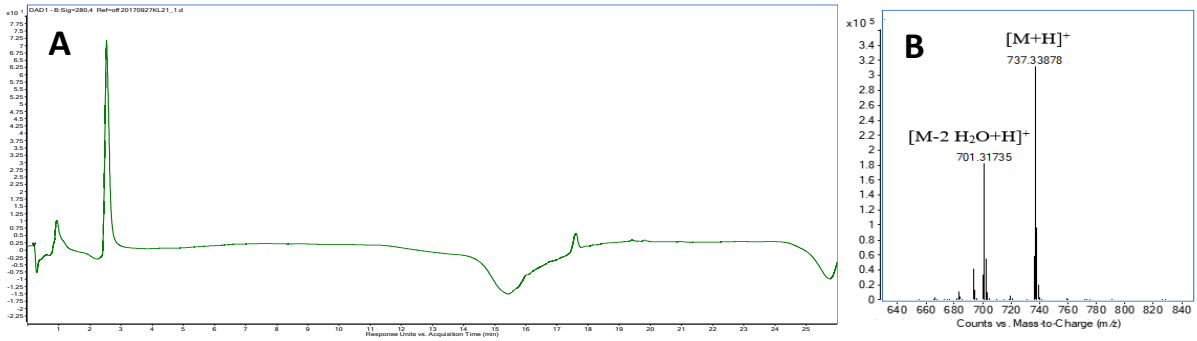

Figure S12. LC trace (A) and mass-spec data (B) of KL21. Water loss is commonly seen upon MS analysis of boronic acid-containing compounds (see Wang et al., *Chem. – Eur. J.* **2013**, *19*, 7587).

KL22

5 was synthesized using standard Fmoc-based SPPS on Rink Amide MBHA resin. It was carried out on a 0.05 mmol synthesis using 5 equivalents of each amino acid and 4.75 equivalents of HBTU for each coupling reaction. $Pd(PPh_3)_4$ (100 mg) and phenylsilane (600 µL) in dichloromethane (2 mL) was added to the resin to selectively deprotect the Alloc group. N^{α}-Fmoc-N^{β}-Boc-L-2,3-diaminopropionic acid was activated with HBTU in 0.4 M *N*-methylmorpholine in dimethylformamide for 3 minutes, then adding the solution to the peptide on-resin and mixing for 1h. After N-terminal Fmoc deprotection with 20% piperidine in dimethylformamide, **9** was cleaved off resin with 90% trifluoroacetic acid : 10% H_2O for 2 hours. Cold ether precipitation yielded crude peptide. A quarter of the crude peptide was dissolved in 100 µL of dimethylformamide. 5 µL of N-methylmorpholine and 5 mg of N-(5-Fluoresceinyl) maleimide was added to the solution. The reaction went for 1h and KL22 peptide was purified using RP-HPLC (Scheme S3). The calculated m/z $[M+H]^+$ is 806.2563 and the observed m/z $[M+H]^+$ is 806.2506 (Figure S13).

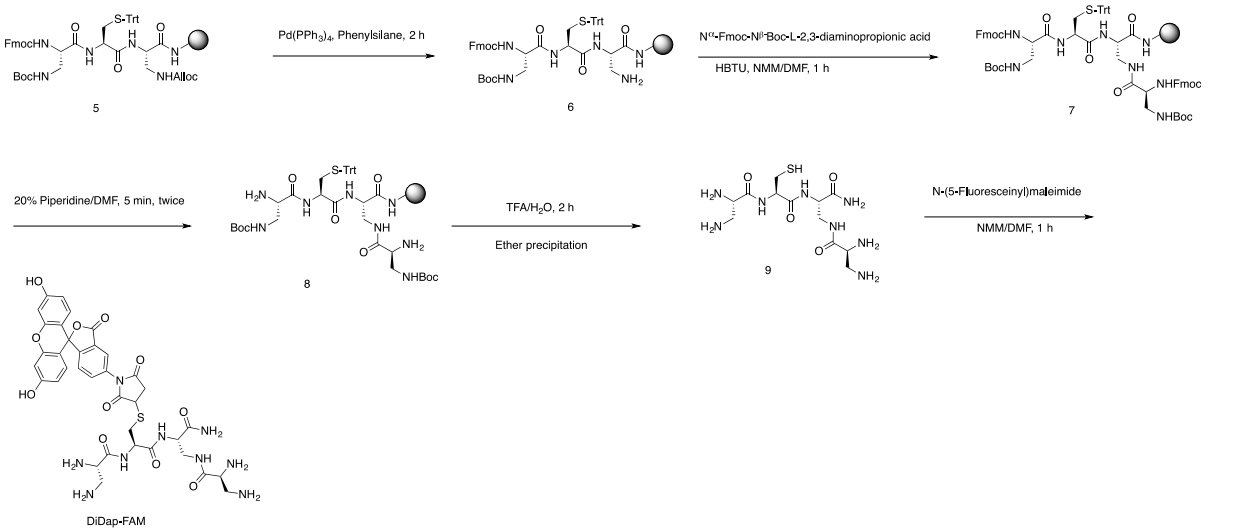

Scheme S3. Synthetic route for KL22.

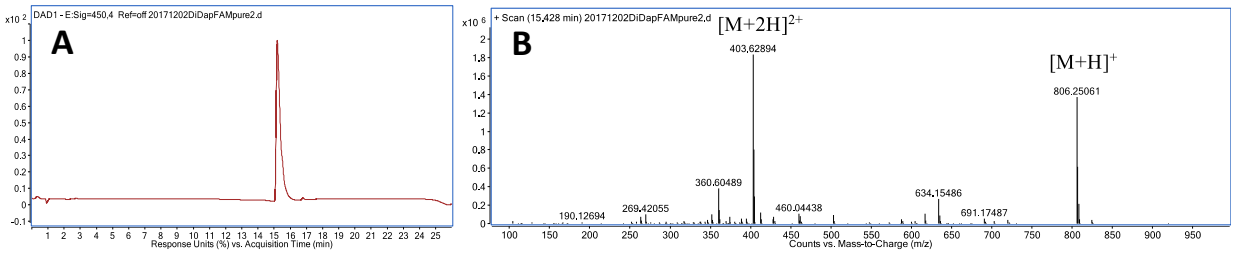

Figure S13. LC trace (A) and mass-spec data (B) of KL22.

KL23

KL23 was synthesized using similar method as KL21.The unnatural amino acid Fmoc-L-Dap-Dabcyl was synthesized through the following method.

Synthesis of Fmoc-L-Dap-Dabcyl

Dabcyl-OSu (50 mg, 0.136 mmol) and Fmoc-L-Dap-OH (44.5 mg, 0.136 mmol) was suspended in 5 mL of dichloromethane. Triethylamine (70 mg, 0.68 mmol) was added to the mixture and the reaction was stirred overnight. 0.02 M HCl (100 mL) was then added to quench the reaction. The product was extracted with ethyl acetate (80 mL × 3). The organic layers were combined, washed with brine (100 mL), and dried over sodium sulfate. The solvent was evaporated and yielded a dark red solid (70 mg, 88% yield). The crude product was directly used for peptide synthesis without further purification (Scheme S4). The calculated m/z $[M\text{-}2H_2O + H]^+$ is 961.3454 and the observed m/z $[M\text{-}2H_2O+H]^+$ is 961.3405 (Figure S14).

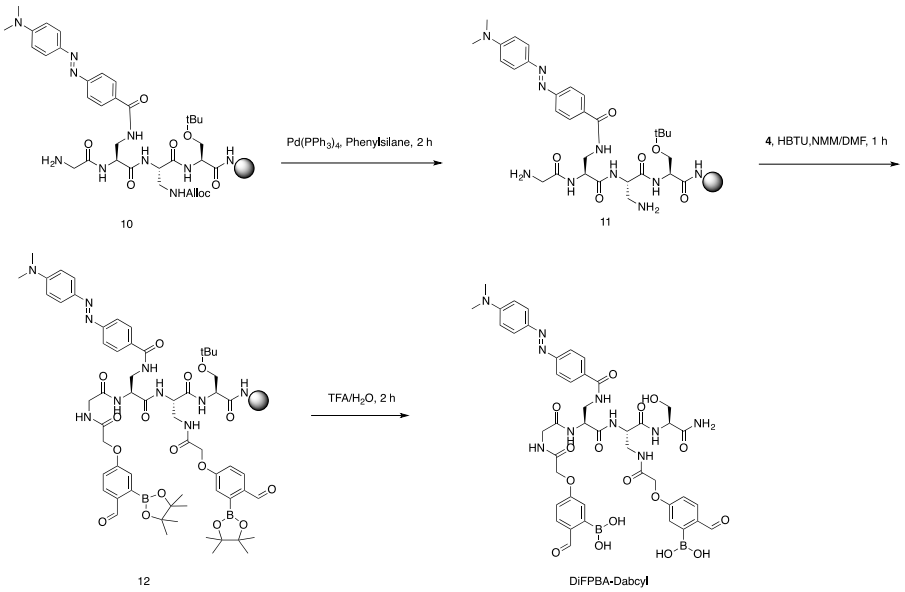

Scheme S4. Synthetic route for KL23.

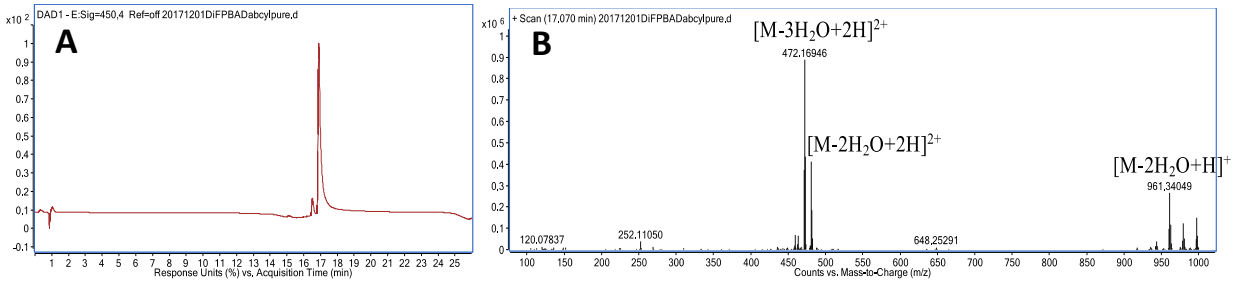

Figure S14. LC trace (A) and mass-spec data (B) of KL23.

17. NMR spectra

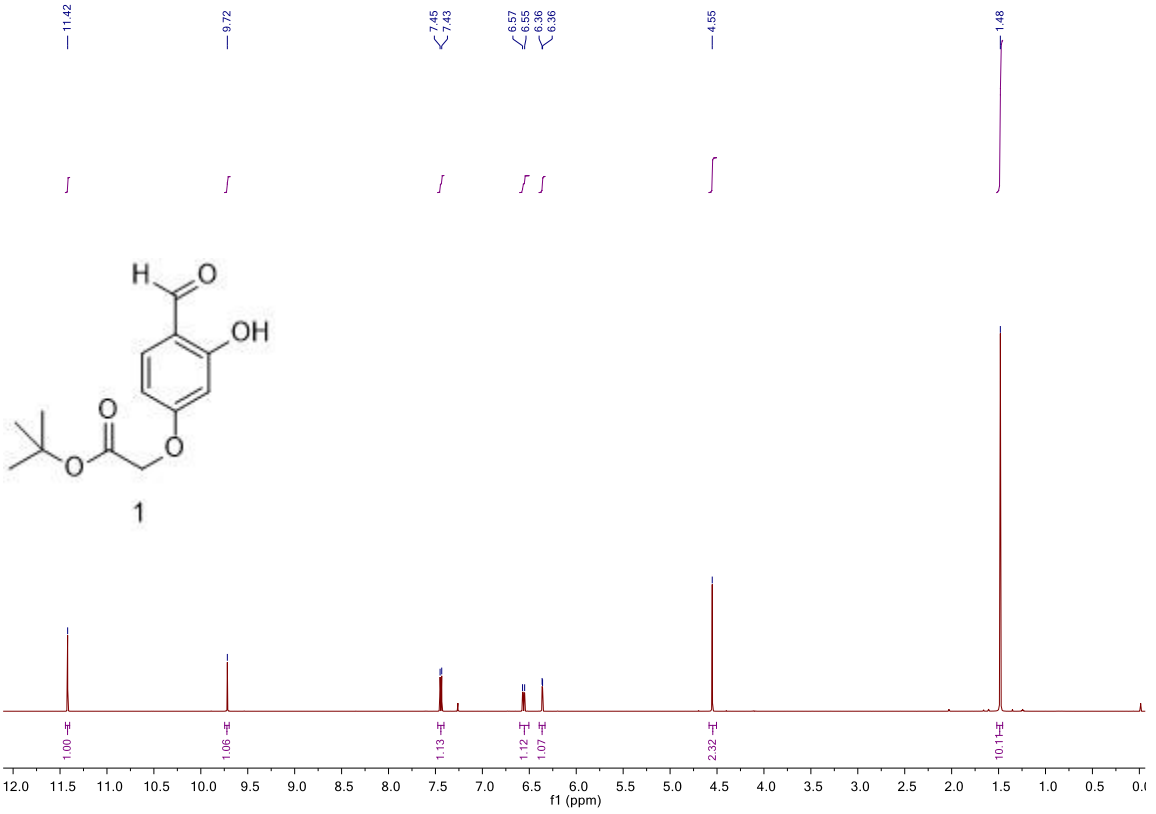

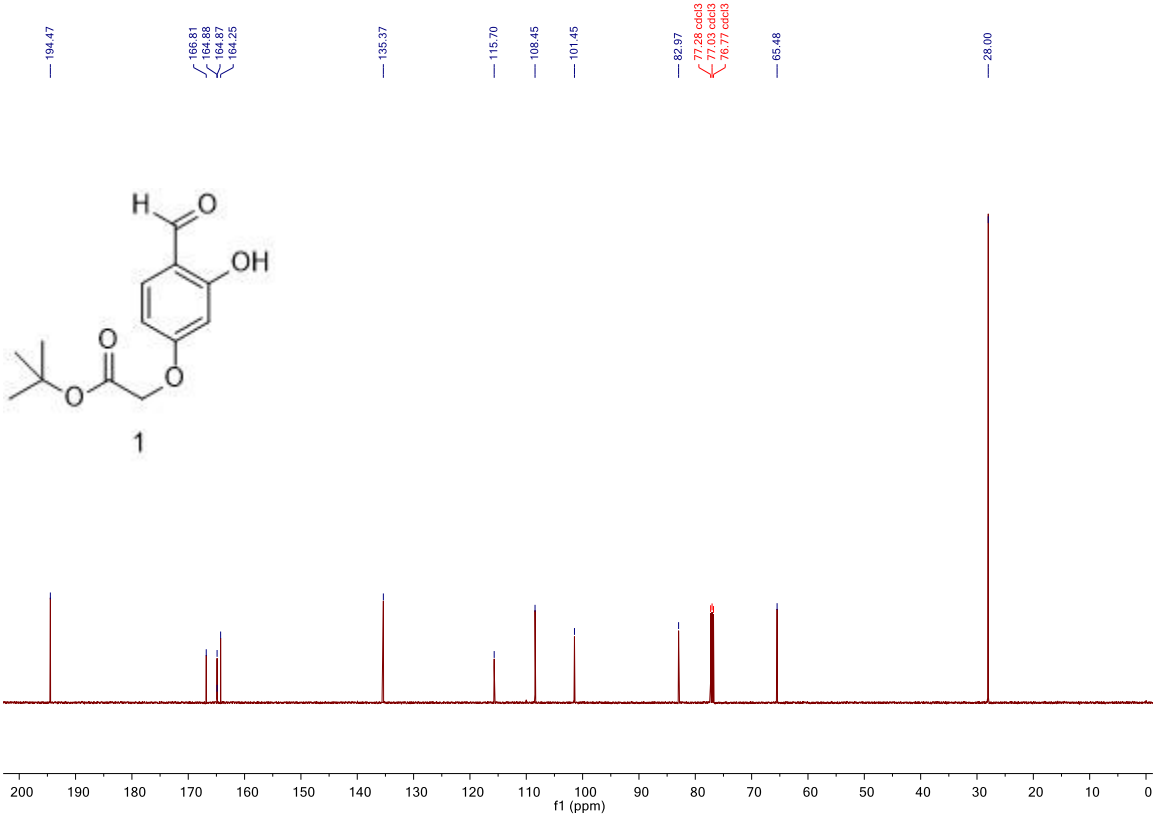

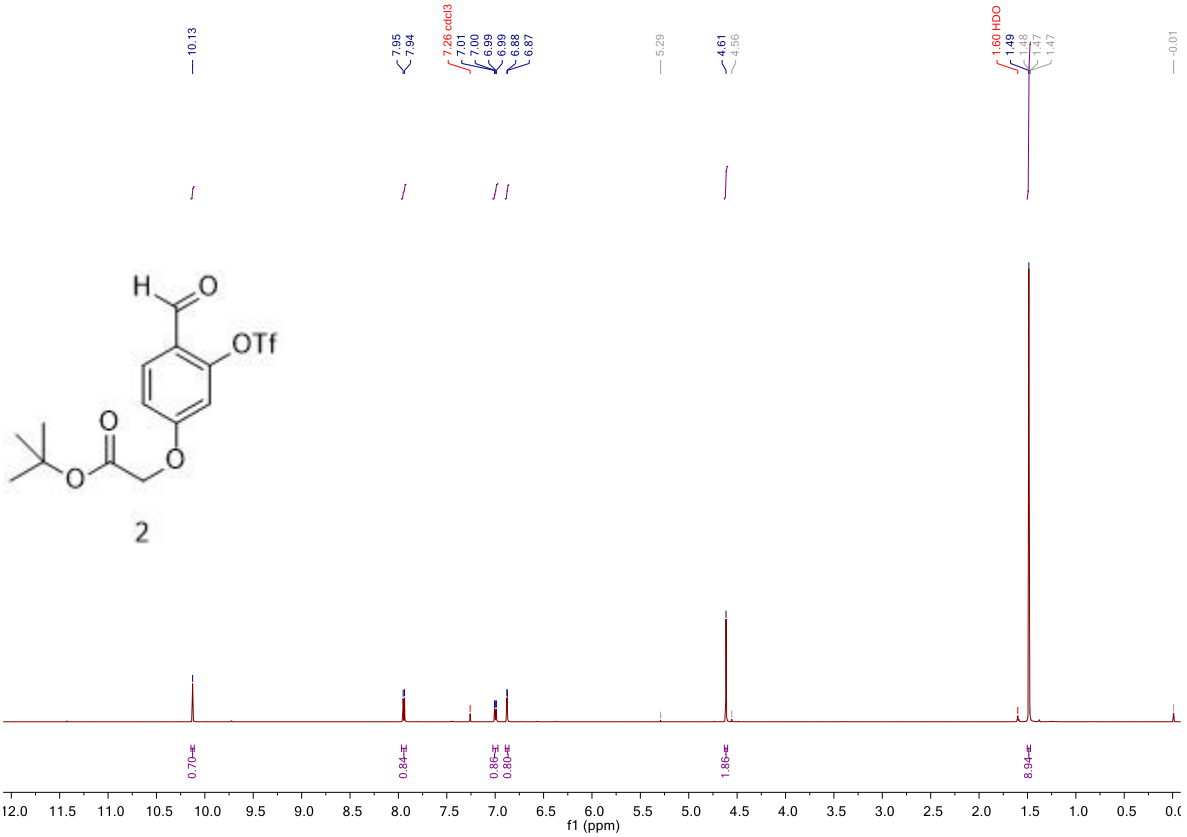
10.13
7.95
7.94
7.26 cdcl3
7.01
7.00
6.99
6.99
6.88
6.87
5.29
4.61
4.56
1.60 HDO
1.49
1.48
1.47
1.47
-0.01
H
O
OTf
O
O
O
2
0.70
0.84
0.86
0.80
1.86
8.94
f1 (ppm)

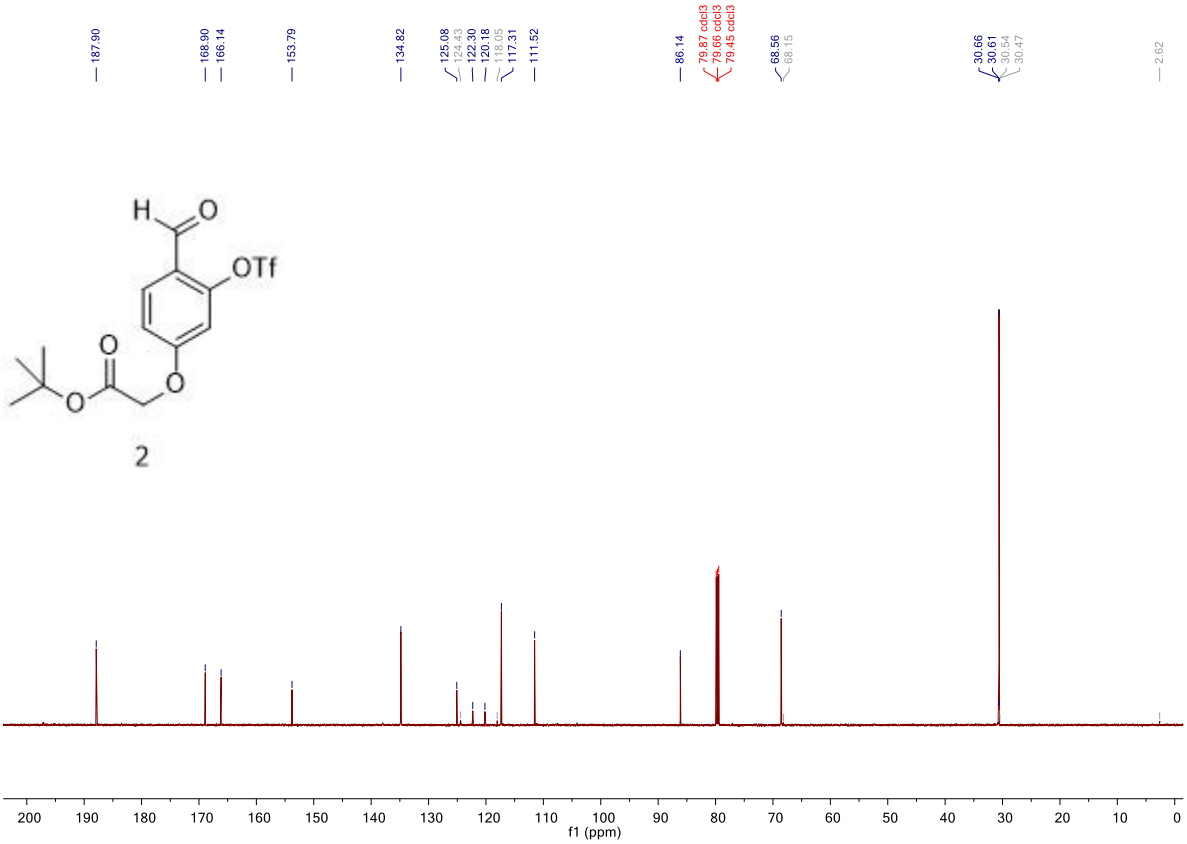
187.90
168.90
166.14
153.79
134.82
125.08
124.43
122.30
120.18
116.05
117.31
111.52
86.14
79.87 cdcl3
79.66 cdcl3
79.45 cdcl3
68.56
68.15
30.66
30.61
30.54
30.47
2.62
H
O
OTf
O
O
O
2
f1 (ppm)

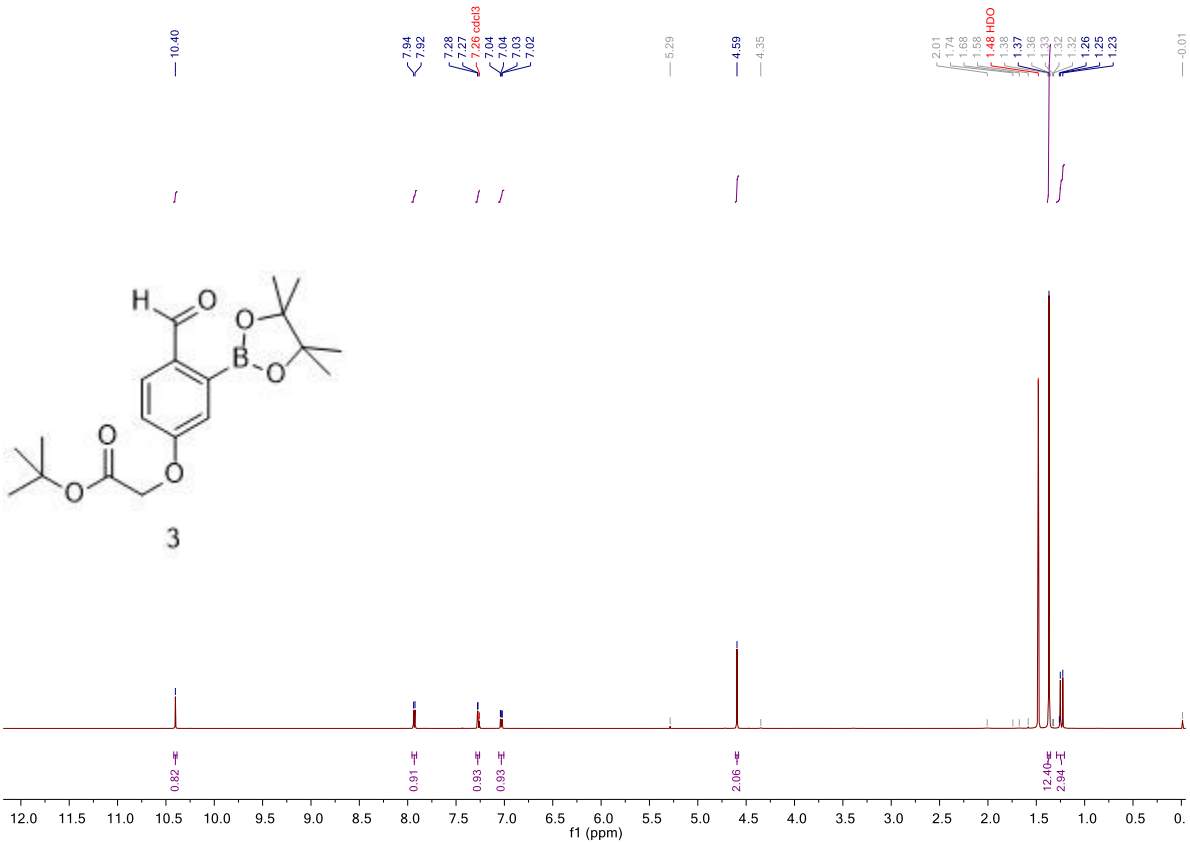
10.40
7.94
7.92
7.28
7.27
7.26 cdcl3
7.04
7.04
7.03
7.02
5.29
4.59
4.35
2.01
1.74
1.68
1.58
1.48 HDO
1.38
1.37
1.36
1.33
1.32
1.32
1.26
1.25
1.23
0.01
H
O
O
B
O
O
O
O
3
0.82
0.91
0.93
0.93
2.06
12.40
2.94
f1 (ppm)

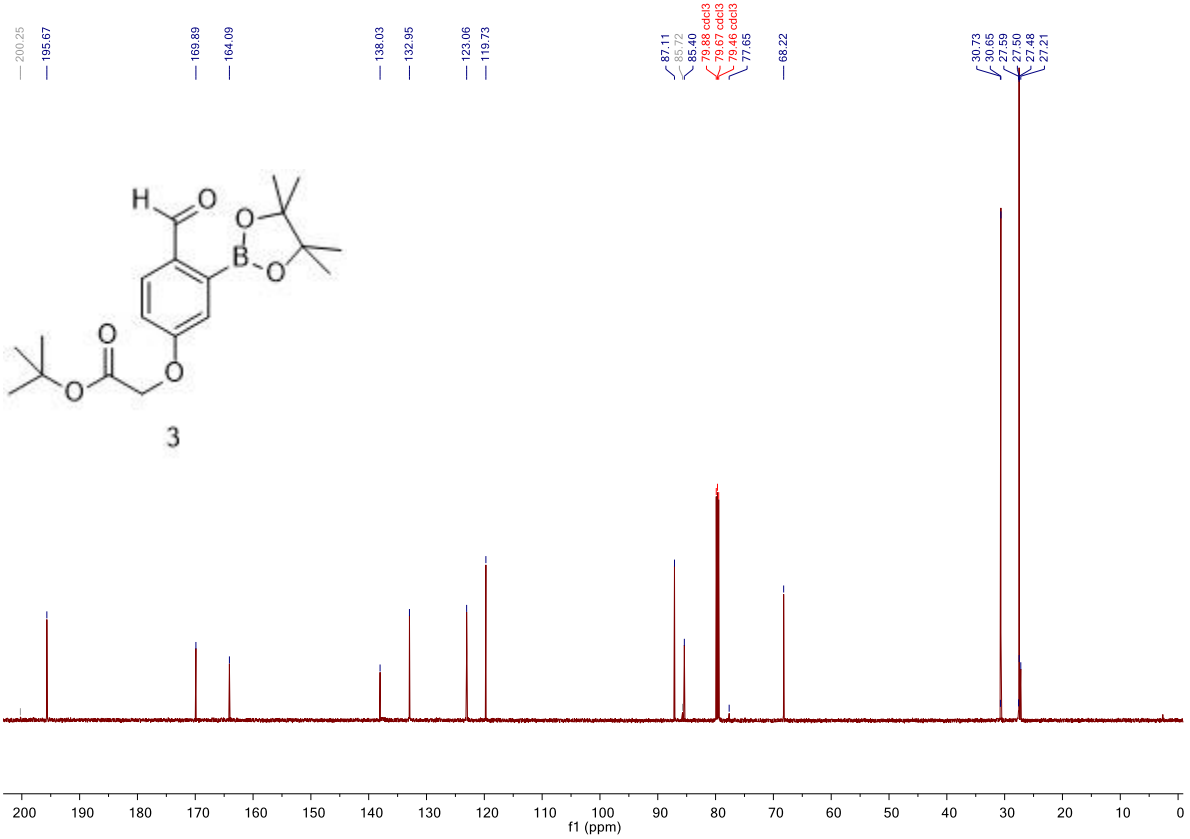
200.25
195.67
169.89
164.09
138.03
132.95
123.06
119.73
87.11
85.72
85.40
79.88 cdcl3
79.67 cdcl3
79.46 cdcl3
77.65
68.22
30.73
30.65
27.59
27.50
27.48
27.21
H
O
O
B
O
O
O
O
3
f1 (ppm)

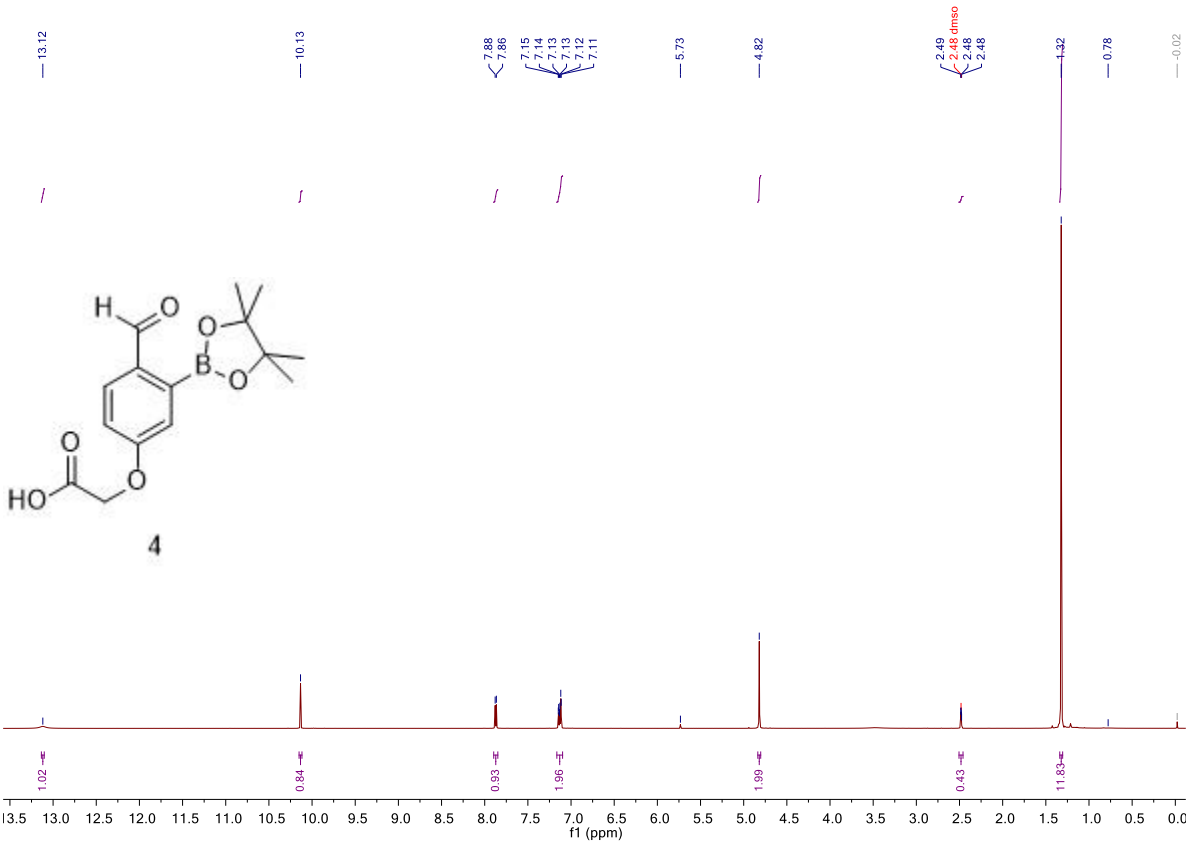
13.12
10.13
7.88
7.86
7.15
7.14
7.13
7.13
7.12
7.11
5.73
4.82
2.49
2.48 dmso
2.48
2.48
1.32
0.78
-0.02
1.02
0.84
0.83
1.96
1.99
0.43
11.83
f1 (ppm)

4

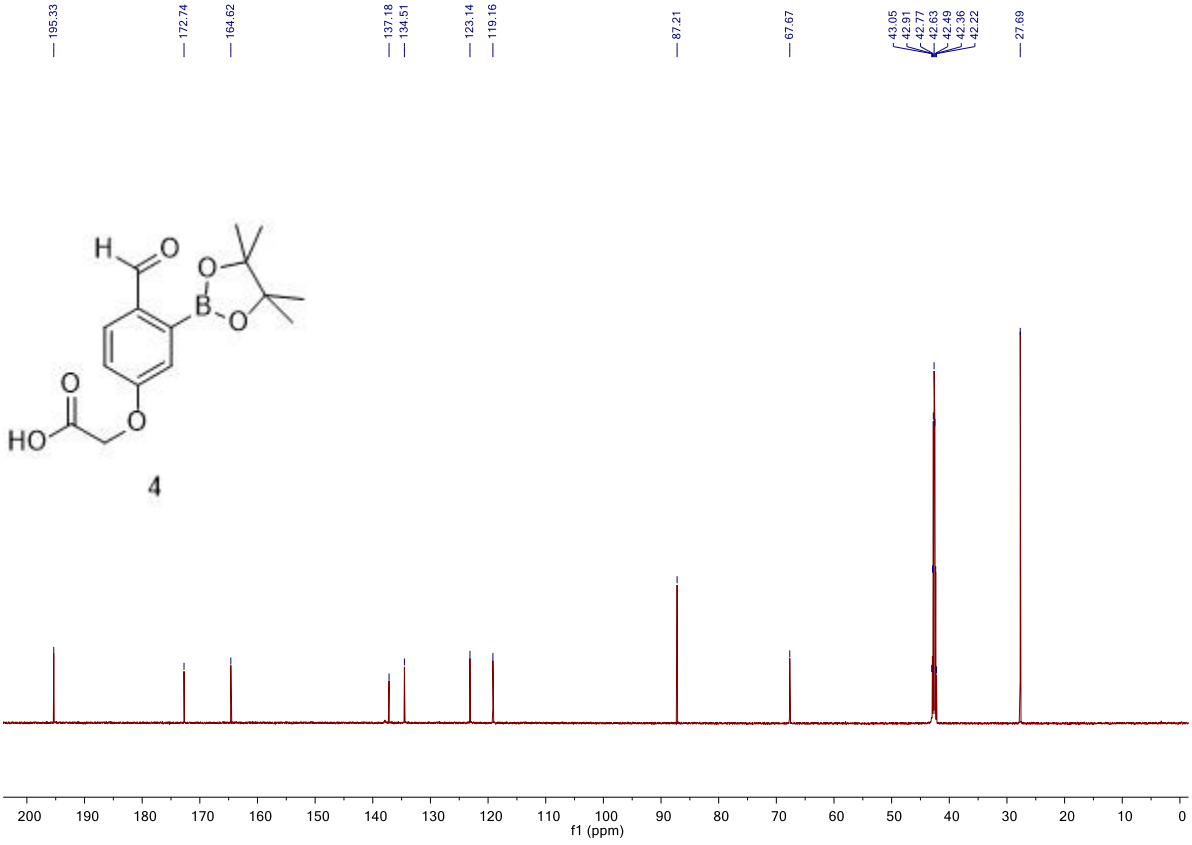
195.33
172.74
164.62
137.18
134.51
123.14
119.16
87.21
67.67
43.05
42.91
42.77
42.63
42.49
42.36
42.22
27.69
f1 (ppm)

4